Ethiopian Journal of Environmental Studies & Management 12(2): 214 – 228, 2019.
ISSN:1998-0507 doi: https://ejesm.org/doi/v12i2.9
Submitted: March 23, 2019 Accepted: May 06, 2019

EMPIRICAL ANALYSIS OF RICE YIELDS DETERMINANT USING REMOTE SENSING VEGETATION HEALTH CONDITION INDICES: CASE STUDY OF LAKE GERIYO, AKERRA AND TALATA-MAFARA, NIGERIA

ALIYU, H.,[1] *BADARU, Y.U.[2] AND ABUBAKAR, A.S.[3]
[1]Nigeria Incentive-Based Risk Sharing System for Agricultural Lending (NIRSAL) PLC, Abuja
[2]Remote Sensing Laboratory, Dept. of Geography, Federal University of Technology, Minna, Nigeria
[3]School of Physical Science, Federal University of Technology, Minna, Nigeria
*Corresponding author: badaruyahayausman@yahoo.com

Abstract
This research focuses on the ability of remote sensing vegetation index acquired from the Landsat-8 operational land imager (OLI)/thematic infrared sensor (TIRS) and Satellite Pour l'Observation de la Terre (SPOT-6 and 7) HRV, HRVIR, HRG system as effective indicator to measure rice growing condition and predicting yield rate. The normalized difference vegetation indices (NDVI), leaf area indices (LAI) and perpendicular vegetation indices (PVI) that embrace supervised and unsupervised application is use to examine dynamics in rice-growing regions, harvest prediction modelling, estimating production yields, determining differences in plant biomass and the assessment of ecosystem services in rice-growing areas. The result shows multivariate regression model correlated nicely with two vegetation indices to produce significant value or classification accuracy of R^2 = 0.3813 (38%) for NDVI, while PVI with significant value of R^2 = 0.3102 (31%). In a normal growing period, the amount of vegetation biomass is at NDVI 0.4550/PVI 0,2227 in the month of December, January, February and March, while, active vegetation at NDVI 0.8225/PVI 0.2882 in the month of May, June, July, August, September and October. Due to the extensively wide range at a rate of NDVI 0.7115-0.8225/PVI 0.2882-0.2960, the areas are favourable for the cultivation of rice. Furthermore, the research is interested in getting the overall value of a vegetation condition for the study areas, therefore, it is clear that a simple mean of the existing data will suffice, since the existing data has high estimate of vegetation across the landscape.

Key Words: *Empirical, yields determinant, Remote sensing, Vegetation condition indices, Vegetation health indices*

Introduction

Agronomic studies have been carried out on various vegetation indices amongst them are NDVI, SAVI, PVI, LAI, DVI, RVI, GVI and EVI, its serve to benefit farmers for the past twenty-five years (Zhang and Kovas, 2012). However, satellite remote sensing (RS) data were

extensively applied to a wide range of research and practical applications (Chang *et al.,* 2016), including rice yield predictions. Zhu *et al*. (2012), used Moderate Resolution Imaging Spectroradiometer Enhanced Vegetation Index (MODIS EVI) time-series data to predict yield in winter crop, revealing a high value. Furthermore, Ali *et al.* (2014) reported continuity of multispectral high-resolution optical observations over global terrestrial surfaces using Sentinel 2, providing detailed information within rice field variability. With the development of super-hyperspectral, hyperspectral and multispectral remote sensing technology (Haboudane, 2004), it is envisioned that these new developments will be readily applied and will become one of the most important to agronomic research in the near future (Mulla, 2013). According to Liu *et al.* (2017), using vegetation indexes is applicable for direct monitoring and diagnosis of rice growth and development, although there might be differences in leaf area index (LAI) and other agronomic parameters.

Aim and Objectives

The basic aim of this research is to examine remote sensing vegetation index (NDVI, PVI and LAI), which has long been applied to measure vegetative development and detect soil reflectance. Therefore, it is logical to hypothesize that it can be an effective indicator of crops growing condition and yields.

The objectives of this study are illustrated as follow:

- Indicate and provide the amount of vegetation (e.g., LAI-percentage cover, RVI and biomass).
- Predicted yield estimation.
- Soil and vegetation reflectance value

Study Areas

The study area comprises of lake Geriyo in Adamawa State of Nigeria, located between the latitudes 09°17'45.87″, 09°17′38.21″ and longitudes 12°26′09.95″, 12°26′24.87″, Akerra in Nasarawa State latitudes 07°52'54.76″, 07°51′05.90″ and longitudes 08°21′48.39″, 08°22′12.73″ and Talata-Mafara located at latitudes 12°37'23.79″, 12°37′36″ and longitudes 06°01′59.92″, 06°02′13.94″ (Figure 1). There are two dominant cropping seasons in the study areas; wet/rainy season begins from April to October, while harvesting in mid-September to October up to November; cool/dry season "harmattan" in which sowing starts from end of November and mid-December, while harvest in February to March.

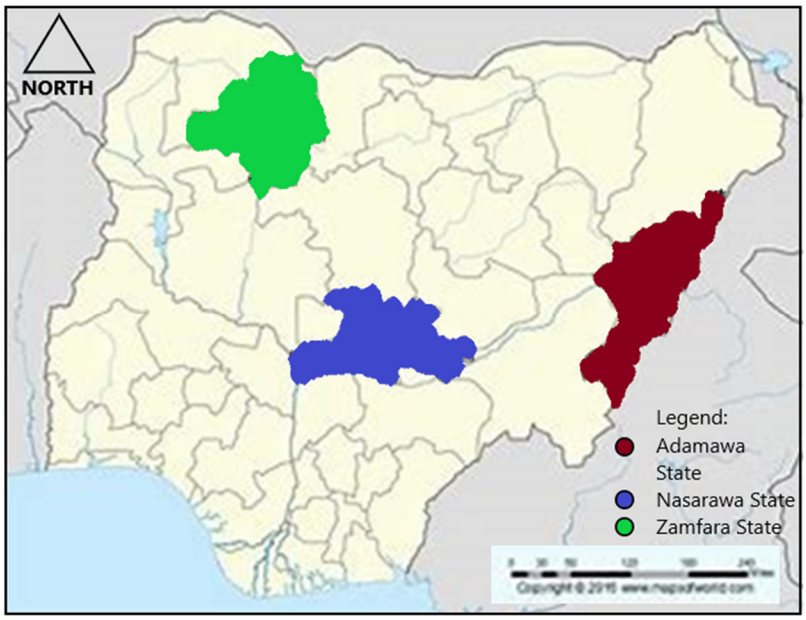

Fig. 1: The study areas.

Literature Review

Yield prediction methods use crop conditions to predict potential yield of rice and maize, thereby determining the value of NDVI and other vegetation indices required (Spitko *et al.,* 2016; Tubana *et al*., 2012). Meanwhile, Liu, *et al.* (2014) and Cao *et al.* (2016) confirmed a relatively stable relationship between NDVI/LAI and grain yield in cropping rice during the growth periods, further described the relationship between NDVI and total nitrogen accumulation from tillering to filling stages, and used the obtained index to predict potential yield and guide nitrogen deposits (Xue *et al.,* 2014; Kanke *et al.,* 2012). NDVI and other vegetation indexes (Liu and Huete, 1995) vary according to crop-age, planting density and chlorophyll activity (Batten, 1998). Satellite images from Landsat, SPOT5, and Quickbird (Anderson *et al.,* 1993) with high spatial resolution of 30 m, 10 m, and 3 m overcame the disadvantage of small survey regions and showed a high level of accuracy for crop yield prediction. Several sensors have been installed on space-borne satellites for crop growth monitoring, crop yield prediction, disease detection (Córcoles *et al.,* 2013; Garcia-Ruiz *et al.,* 2013; Hunt *et al*., 2005; Mahlein, 2013), and monitor plant growth and biochemical indicators for many vegetation indices (Li *et al*., 2012; Zarco-Tejada *et al.,* 2012; Verger *et al.,* 2014). However, studies have shown that NDVI, PVI and LAI (Li *et al*., 2015; Richardson and Wiegand, 1977) have a significant saturation effect under high vegetation coverage (Shaver *et al*., 2010), in rice, accuracy decreases when the leaves are dry, increases when the leaves matter is green (Yao *et al*., 2013).

Methods

Landsat-8 OLI/TIRS and SPOT-6 & 7 HRV, HRVIR, HRG images taken on two different farming seasons (10/2017 and 12/2018) were visually and digitally analysed to measure rice cultivated area

using NDVI, LAI and PVI. Band combination was selected as an appropriate subset in the digital analysis for the estimation of rice areas. An attempt was made to develop a relationship between reflectance values and actual yield using an image of the fully ripened stage of the crop. In calculating the NDVI, LAI and PVI of a surface with vegetation, the reflectance in the red and NIR ranges are measured and plotted on a graph. PVI measures the changes from the bare soil reflectance caused by the vegetation. In this way it gives an indication of vegetative cover independent of the effects of the soil. The LAI measures the extent of the vegetation areas, while NDVI measures the potentials of greenness. This was used for estimating yield per hectares.

Results

NDVI/LAI at Talata-Mafara

Figure 2 shows rice plant vegetation cycle throughout the study areas. It is also clear that the existing satellite data is discriminated across the landscape of 2km^2 or 200 hectares. The healthy leaves areas are dark green, while, areas with little or no vegetation are bright-gold, meaning the portion of reflected near-infrared light depends on the cell structure of the leaf, therefore, fading or unhealthy leaves, photosynthesis decreases and cell structure collapses resulting in an increase of reflected visible light and a decrease of reflected near infrared light. NDVI (greenness) is calculated from these individual measurements as follows:

NDVI = (NIR –Red)/ (NIR+Red)

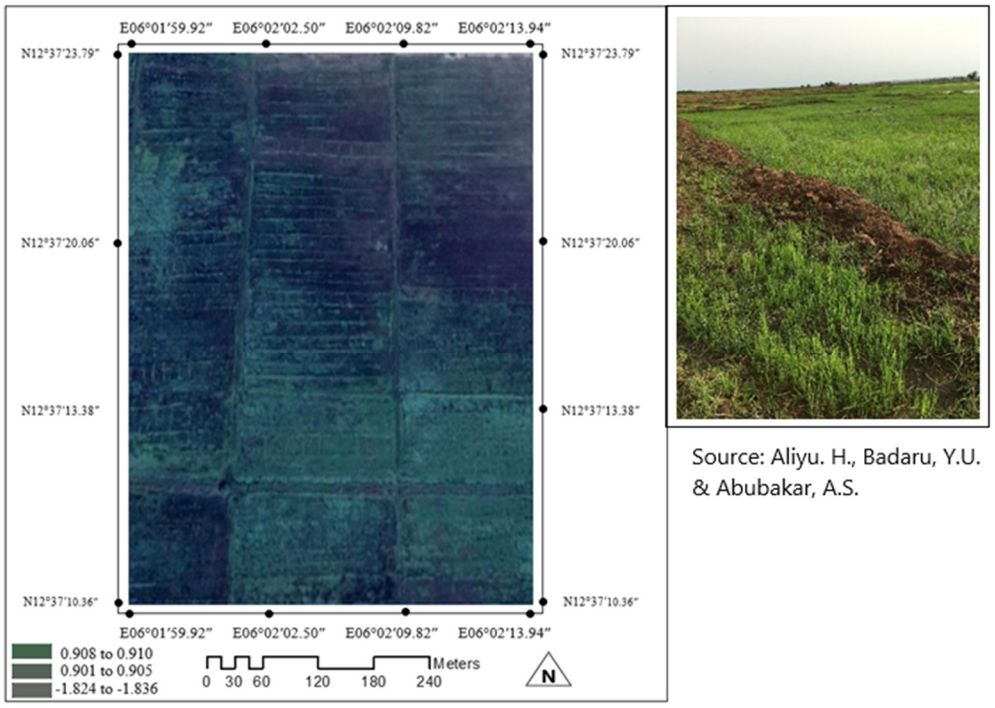

Source: Aliyu. H., Badaru, Y.U. & Abubakar, A.S.

Fig. 2: The distribution of real-time imagery of rice cultivated areas at Talata-Mafara

Figure 3 shows the value of rice biomass for different NDVI threshold value. Empirical study implies that the value of NDVI is found to be 31.24% at NDVI threshold of 0.7680 (pixel-2), 33.91% at NDVI threshold of 0.8336 (pixel-3), 34.85% at NDVI threshold of 0.8566 (pixel-4), while, LAI of active

agricultural area is found to be 41.57% (healthy) and remaining area is found to be unhealthy plant 58.43%. The NDVI and LAI method gives superior results for vegetation varying in densities and also for scattered vegetation from a multispectral remote sensing image.

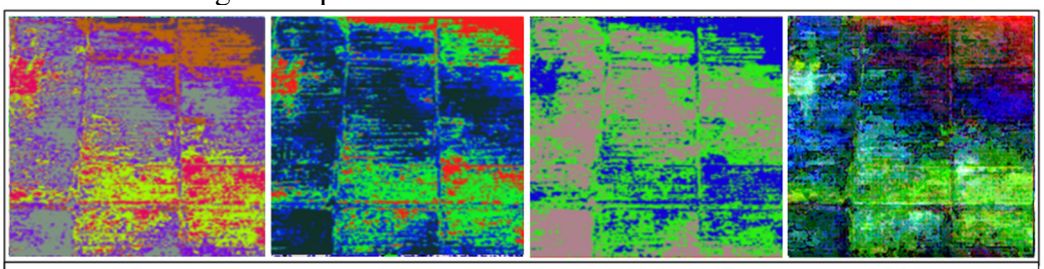

Pixel-1	Pixel-2	Pixel-3	Pixel-4
NDVI = *f*NIR-*f*R/*f*NIR+*f*R	NDVI = *f*NIR-*f*R/*f*NIR+*f*R	NDVI = *f*NIR-*f*R/*f*NIR+*f*R	NDVI = *f*NIR-*f*R/*f*NIR+*f*R
-	*0.7680*	*0.8336*	*0.8566*

Fig. 3: NDVI of vegetation reflectivity of colour, roughness and water content NDVI/LAI at Lake Geriyo

Figure 4 shows that the healthy rice leaves areas are dark-green, while, areas with little or no vegetation are bright-gold. In the fixed effect case, each plot of 1.0 hectare is assumed to have dissimilar intercept terms as reflected in the subscript. On the other hand, the random effect reflected assumes that all reflectance values of the total plot of 4.5km^2 or 450 hectares are reflected in the similar term.

NDVI = (NIR –Red)/ (NIR+Red)

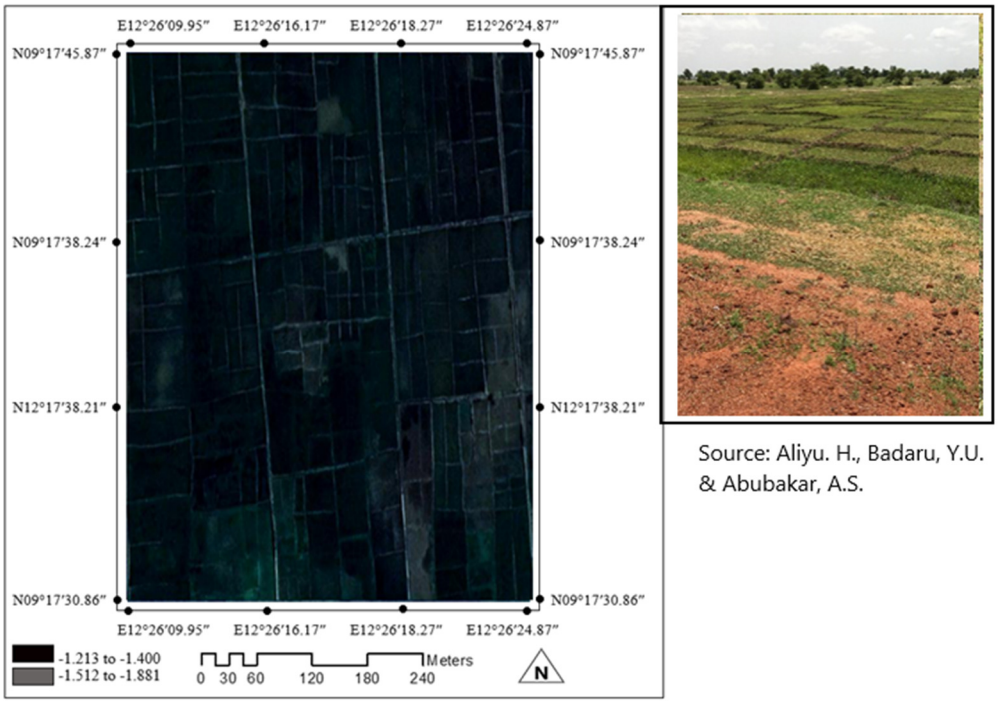

Source: Aliyu. H., Badaru, Y.U. & Abubakar, A.S.

Fig. 4: The distribution of real-time imagery of rice cultivated areas at Lake Geriyo

Figure 5 implies that the value of NDVI is found to be 22.74% at NDVI threshold of 0.7115 (pixel-1), 25.45% at NDVI threshold of 0.7960 (pixel-2), 25.55% at NDVI threshold of 0.7992 (pixel-3), 26.26% at NDVI threshold of 0.8215 (pixel-4), while, LAI of active agricultural area is found to be 78.19% healthy and remaining area is found to be unhealthy 21.81%. The NDVI and LAI method gives superior results for vegetation varying in densities and also for scattered vegetation from a multispectral remote sensing image.

Pixel-1	Pixel-2	Pixel-3	Pixel-4
NDVI = $fNIR\text{-}fR/fNIR+fR$	NDVI = $fNIR\text{-}fR/fNIR+fR$	NDVI = $fNIR\text{-}fR/fNIR+fR$	NDVI = $fNIR\text{-}fR/fNIR+fR$
0.7115	*0.7960*	*0.7992*	*0.8215*

Fig. 5: NDVI of vegetation reflectivity of colour, roughness and water content

NDVI/LAI at Akerra

As can be seen from the Figure 6, the changes in rice plant vegetation biomass were easily observed. In the images of 2km^2 or 200 hectares, the green areas represent the healthy and vegetated areas, the off-white areas represent the non-vegetated areas (footpaths and Irrigation routes), and the light-gold areas represent the low-vegetated areas. So, this can be concluded that the area is highly vegetated.

NDVI = (NIR –Red)/ (NIR+Red)

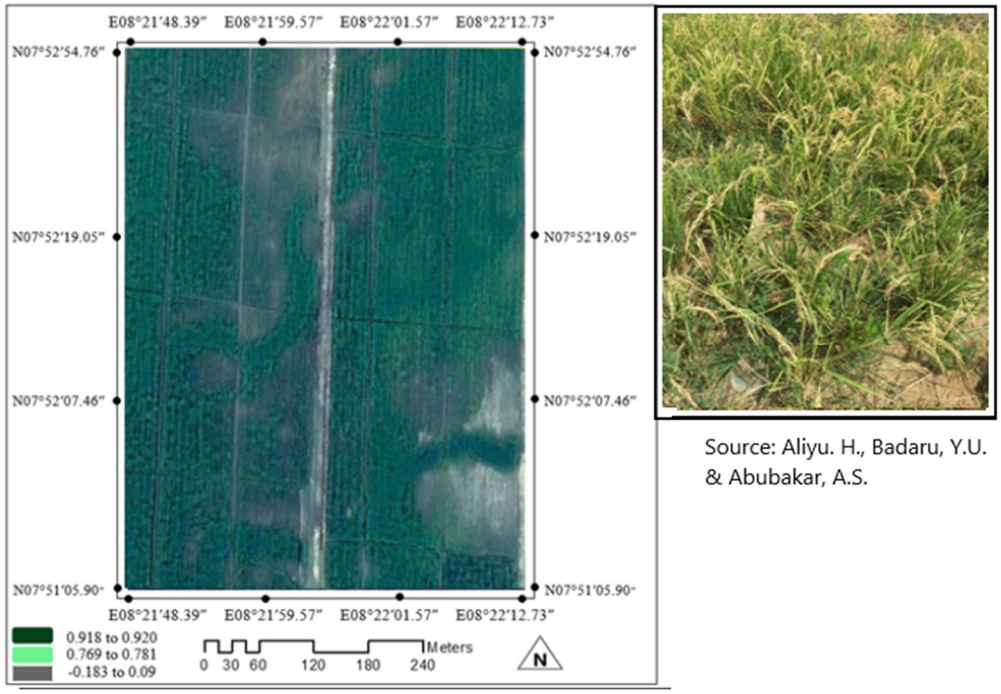

Source: Aliyu. H., Badaru, Y.U. & Abubakar, A.S.

Fig. 6: The distribution of real-time imagery of rice cultivated areas at Akerra

Figure 7 clearly shows that the value of NDVI is found to be 22.367% at NDVI threshold of 0.7128 (pixel-1), 25.041% at NDVI threshold of 0.7980 (pixel-2), 26.861% at NDVI threshold of 0.8560 (pixel-3), 25.731% at NDVI threshold of 0.8200 (pixel-4), while, LAI of active agricultural area is found to be 52.86% healthy and remaining area is found to be unhealthy 47.14%. The NDVI and LAI method gives superior results for vegetation varying in densities and also for scattered vegetation from a multispectral remote sensing image.

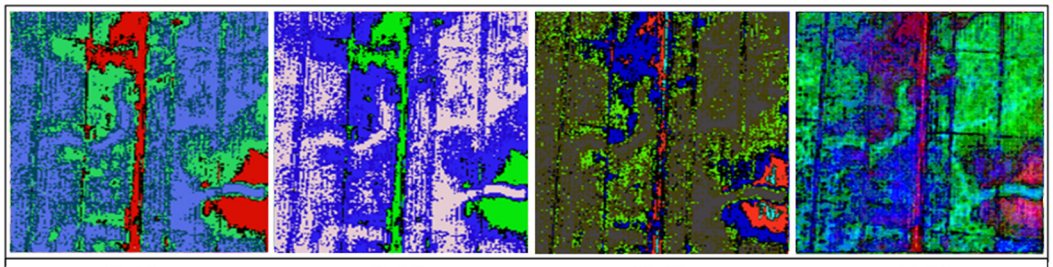

Pixel-1	Pixel-2	Pixel-3	Pixel-4
NDVI = *f*NIR-*f*R/*f*NIR+*f*R	NDVI = *f*NIR-*f*R/*f*NIR+*f*R	NDVI = *f*NIR-*f*R/*f*NIR+*f*R	NDVI = *f*NIR-*f*R/*f*NIR+*f*R
0.7128	*0.7980*	*0.8560*	*0.8200*

Fig. 7: NDVI of vegetation reflectivity of colour, roughness and water content.

PVI/LAI at Talata-Mafara

Figure 8 shows changes in rice plant pattern across the satellite image of 2km^2 or 200 hectares of a particular part of the landscape. In the image, the green areas represent the healthy vegetation areas and the light-gold areas represent the low-vegetated areas. It is clear that there is a lot of variation across the landscape. PVI is calculated from these individual measurements as follows:

PVI = $\sqrt{(f\text{soil}-f\text{veg})^2 - (f\text{soil}-f\text{veg})^2}$ and NIR = -sin a (NIR) cos a (red)

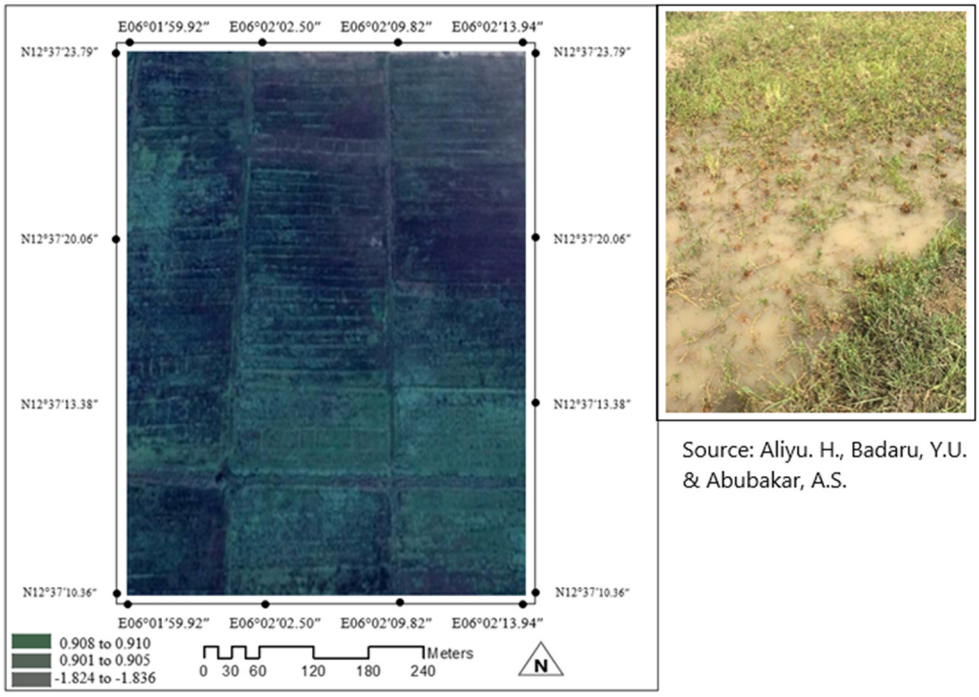

Fig. 8: The distribution of real-time imagery of rice cultivated areas at Talata-Mafara

Figure 9 indicates that the value of PVI is found to be 20.89% at PVI threshold of -0.2140 (pixel-1), 26.13% at PVI threshold of -0.2677 (pixel-2), 24.09% at PVI threshold of -0.2468 (pixel-3), 28.89% at PVI threshold of -0.2960 (pixel-4), while, LAI of active agricultural area is found to be 84.76% healthy and remaining area is found to be unhealthy 15.24%. The PVI and LAI method gives superior results for vegetation varying in densities and also for scattered vegetation from a multispectral remote sensing image.

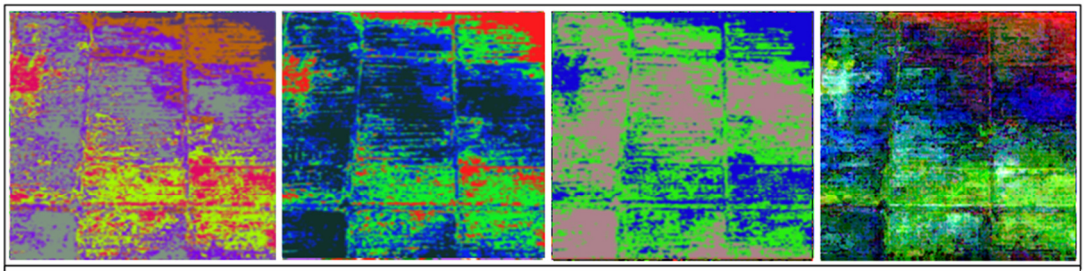

Pixel-1	Pixel-2	Pixel-3	Pixel-4
PVI = √($f$soil-$f$veg)² - ($f$soil-$f$veg)²	PVI = √($f$soil-$f$veg)² - ($f$soil-$f$veg)²	PVI = √($f$soil-$f$veg)² - ($f$soil-$f$veg)²	PVI = √($f$soil-$f$veg)² - ($f$soil-$f$veg)²
-0.2140	-0.2677	-0.2468	-0.2960

Fig. 9: PVI of soil reflectance and vegetation reflectivity

PVI/LAI at Lake Geriyo

Figure 10 clearly shows rice plant vegetation distribution pattern across the satellite imagery of 4.5km^2 or 450 hectares. The satellite data are biased towards southern parts of the landscape. Therefore, the imagery indicates certain areas are much more vegetated than others, for example, the healthy leaves areas are dark-green, and areas with little or no vegetation are bright-gold. More importantly, each plot is assumed to have dissimilar intercept terms as reflected in the imagery, the random effect reflected assumes that all reflectance values of each plot are reflected in the similar way.

PVI = $\sqrt{(f\text{soil}-f\text{veg})^2} - (f\text{soil}-f\text{veg})^2$ and NIR = -sin a (NIR) cos a (red)

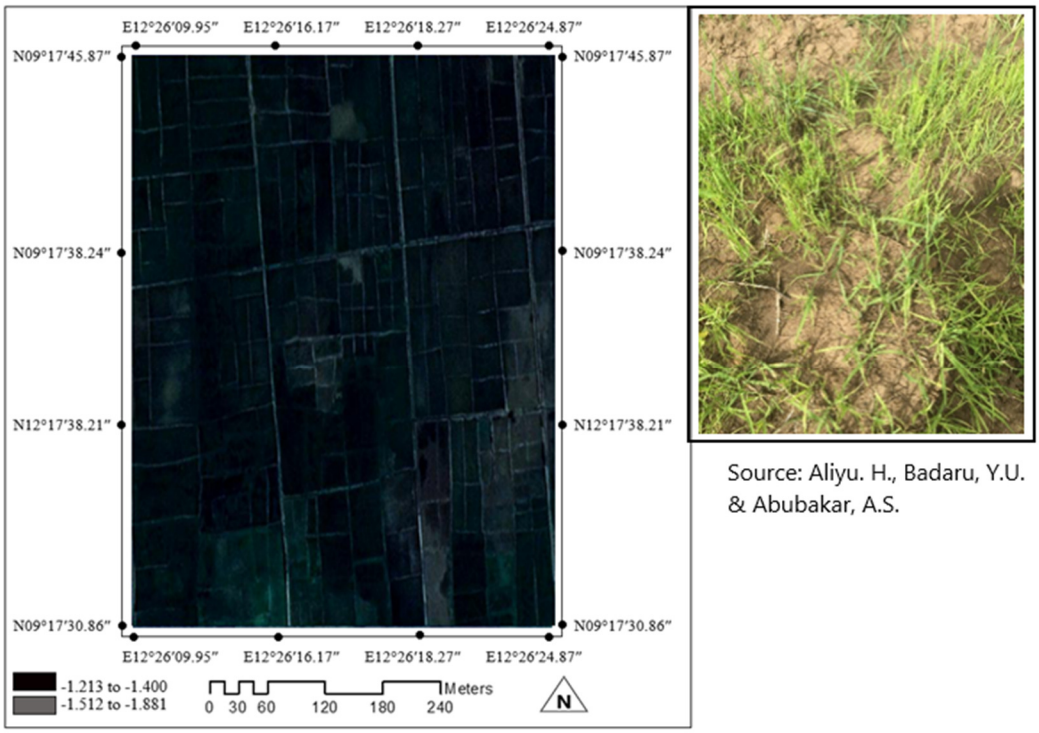

Fig. 10: The distribution of real-time imagery of rice cultivated areas at Lake Geriyo

Empirical study implies that the value of PVI is found to be 35.06% at PVI threshold of -0.2570 (pixel-2), 32.4693% at PVI threshold of -0.2380 (pixel-3), 32.4794% at PVI threshold of -0.2380 (pixel-4), while, LAI of active agricultural area is found to be 81.15% healthy and remaining area is found to be unhealthy 18.85%. The PVI and LAI method gives superior results for vegetation varying in densities and also for scattered vegetation from a multispectral remote sensing image (Figure 11).

Pixel-1	Pixel-2	Pixel-3	Pixel-4
PVI = √($f$soil-$f$veg)² - ($f$soil-$f$veg)²	PVI = √($f$soil-$f$veg)² - ($f$soil-$f$veg)²	PVI = √($f$soil-$f$veg)² - ($f$soil-$f$veg)²	PVI = √($f$soil-$f$veg)² - ($f$soil-$f$veg)²
-	-0.257	-0.238	-0.238

Fig. 11: PVI of soil reflectance and vegetation reflectivity

PVI/LAI at Akerra

Figure 12 shows that the most densely vegetated rice plant areas are green, and areas with little or no vegetation are bright-gold. The imagery (2km^2 or 200 hectares) indicates certain areas are much more heavily vegetated than others (Figure 12), therefore, it is clear

that a simple mean of the existing data will suffice, since the existing data has high estimate of vegetation across the landscape.

PVI = $\sqrt{(f\text{soil}-f\text{veg})^2 - (f\text{soil}-f\text{veg})^2}$ and NIR = -sin a (NIR) cos a (red)

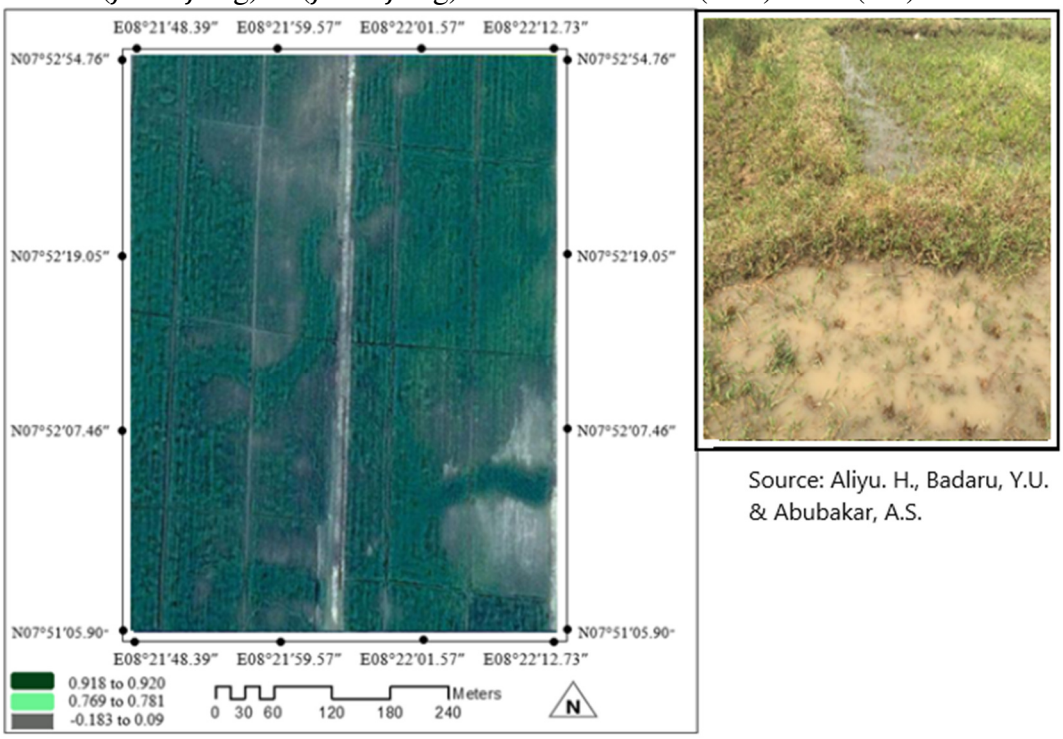

Fig. 12: The distribution of real-time imagery of rice cultivated areas at Akerra.

Figure 13 shows that the value of PVI is found to be 27.599% at PVI threshold of -0.2227 (pixel-1), 35.717% at PVI threshold of -0.2882 (pixel-3), 36.684% at PVI threshold of -0.2960 (pixel-4), while, LAI of active agricultural area is found to be 74.49% healthy and remaining area is found to be unhealthy 25.51%. The PVI and LAI method gives superior results for vegetation varying in densities and also for scattered vegetation from a multispectral remote sensing image.

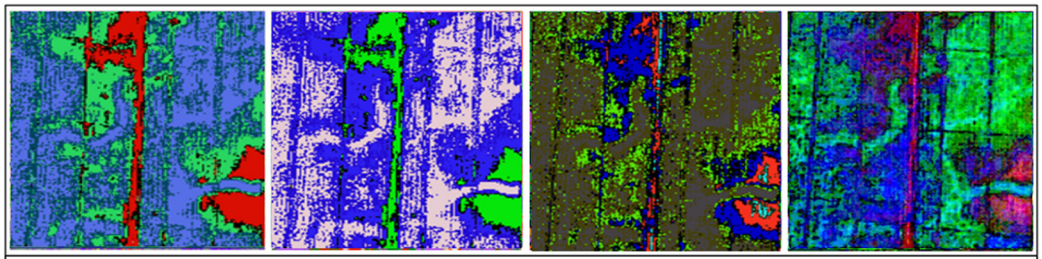

Pixel-1	Pixel-2	Pixel-3	Pixel-4
PVI = $\sqrt{(f\text{soil}-f\text{veg})^2 - (f\text{soil}-f\text{veg})^2}$	PVI = $\sqrt{(f\text{soil}-f\text{veg})^2 - (f\text{soil}-f\text{veg})^2}$	PVI = $\sqrt{(f\text{soil}-f\text{veg})^2 - (f\text{soil}-f\text{veg})^2}$	PVI = $\sqrt{(f\text{soil}-f\text{veg})^2 - (f\text{soil}-f\text{veg})^2}$
-0.2227	-	-0.2882	-0.2960

Fig. 13: PVI of soil reflectance and vegetation reflectivity

NDVI Multivariate Analysis

The statistics of rice yields indicators from October 2017 to December 2018 are presented in Figure 14. There was a lot of variation for yields indicators, with a mean of 0.8194 per 200 hectares and a standard deviation of 58.43% (Talata-Mafara), 0.78205 per 450 hectares and a standard deviation of 21.81% (Lake-Geriyo)) and 0.7967 per 200 hectares and a standard deviation of 47.14% (Akerra). The predicted lowest yield was 41.5% (NDVI 0.7680) per 200 hectares at Talata-Mafara and the highest was 78.19% per 450 hectares at Lake-Geriyo. Therefore, the statistically regression result of NDVI shows significant value or classification accuracy of $R^2 = 0.3813$ (38%).

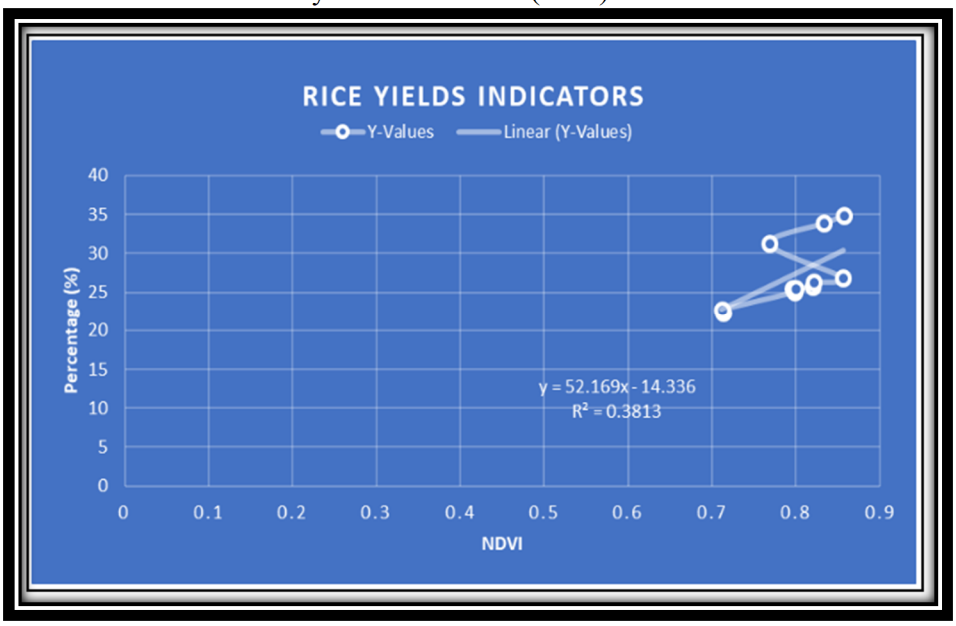

Fig. 14: The regression values of rice yields indicators

PVI Multivariate Analysis

The statistics of rice yields indicators from October 2017 to December 2018 are presented in Figure 15 for the study areas. There was a lot of variation for yields indicators, with a mean of -0.256125 (2.56×10^{-1}) per 200 hectares and a standard deviation of 15.24% (Talata-Mafara), -0.244333 (2.44×10^{-1}) per 450 hectares and a standard deviation of 18.85% (Lake-Geriyo)) and -0.268966 (2.68×10^{-1}) per 200 hectares and a standard deviation of 25.51% (Akerra). The predicted lowest yield was 74.49% (PVI -0.2960) per 200 hectares at Akerra and the highest was 84.76% per 200 hectares at Talata-Mafara. Therefore, the statistically regression result of PVI shows significant value or classification accuracy of $R^2 = 0.3102$ (31%).

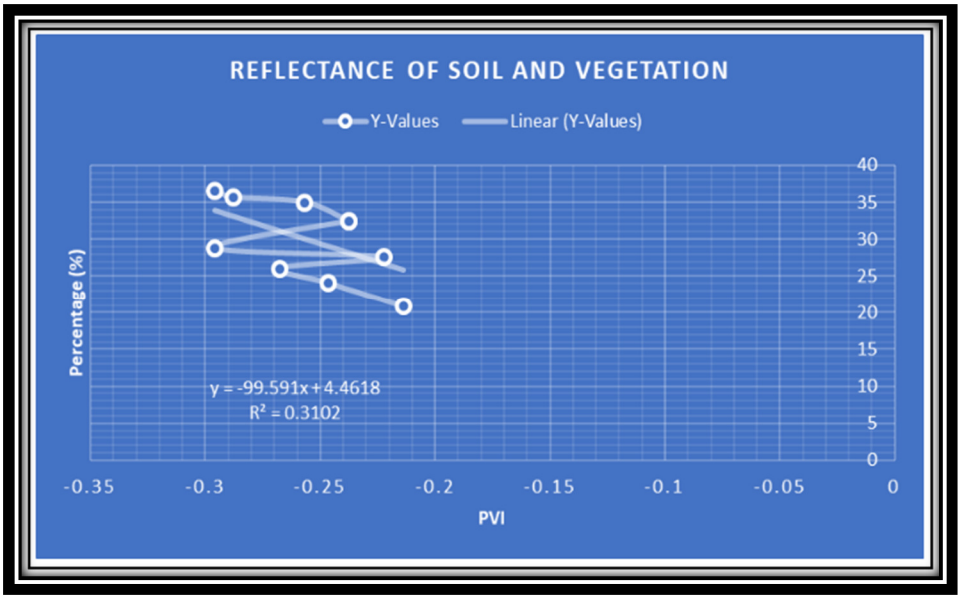

Fig. 15: The regression value of soil and vegetation reflectance.

Discussion

The ability of remote sensing to rapidly predict crop yields in real time is an area of active research investigated. The study examines how the applications of vegetation indices (VIs), such as NDVI, PVI and LAI, in rice yield prediction shows good prediction accuracy. In this study, the relationships between grain yield and the identification index from digital images were studied at different growth stages based on images taken by Landsat. Results shows that with the help of vegetation indices from different satellite images, the spatial distribution of vegetation could be detected and vulnerable areas highlighted. Attention has to be given to rice areas with low and high plant response with respect to soil properties reflectance. The report of the result also shows NDVI, PVI and LAI provide insight into the development of rice biomass in a selected area. It's essential to note that, healthier plants with more chlorophyll have lower reflectance in blue and red wavelengths. Also, healthier plants have a more robust leaf structure which results in higher near-infrared reflectance. The result also shows that the terrain or landscape has gain (66.4%) and loss (33.6%) as a result of gravitation level on cultivated land, with 72.5% part covered with greenness rice plant and 27.5% covered with yellowish or less vegetation. It is important to note that NDVI, PVI and LAI do distinguish between rice types, cultivated areas and the pattern of natural vegetation of which healthy rice crops appear green or greenness in a real-colour simulated image. As shown in Figure 3,5,7,9,11 and 13, the darker areas are dry bare land with minimal vegetation. The processed vegetation indices images help identify vulnerable areas. In addition, knowledge of the rice crop and location of growing areas has help analyse the images and trace vegetation that might be affected by a loss of vegetation vigor.

Conclusions

We determined that the addition of vegetation parameters and other remotely sensed parameters to NDVI, PVI and LAI

increased the explanatory power of our research, and that the best models to predict rice yields abundance include vegetation metrics with remote sensing techniques. We can conclude that in general, healthy rice species increase with higher NDVI, PVI and much more total cover/LAI. In addition, the presence of water with less Total Dissolved Solid (TDS) also resulted in an increase in rice abundance. Our data also demonstrate that more rice exist in areas where NDVI and LAI value is high and PVI value is low with less canopy cover. This finding reinforces the importance of remote sensing for conserving and re-establishing precision agriculture. Remote sensing has become a new platform for acquiring high spatio-temporal resolution images used for precision agriculture. This study has demonstrated that both multispectral and digital images acquired are reliable for rice growth and grain yield estimation.

Acknowledgements

This study would not have been possible without the assistance by the Nigeria Environmental Society (NES) and ISU Remote Sensing Algorithms (ISU-RSAL). We sincerely acknowledge their support. We are grateful to farmer's respondents who also made this study a success.

References

Ali, A.M., Thind, H.S., Sharma, S. and Varinderpal-Singh (2014). Prediction of dry direct-seeded rice yields using chlorophyll meter, leaf colour chart and GreenSeeker optical sensor in north-western India. *Field Crops Res*., 161: 11–15.

Anderson, G.L., Hanson, J.D., and Haas, R.H. (1993). Evaluating Landsat thematic mapper derived vegetation indices for estimating above-ground biomass on semiarid rangelands. *Remote Sensing of the Environment,* 45(2):165-175.

Batten, G.D. (1998). "Plant analysis using near infrared reflectance spectroscopy: The potential and the limitations," *Australian Journal of Experimental Agriculture*, 38(7): 697–706.

Cao, Q., Miao, Y., Shen, J., Yu, W., Yuan, F., Cheng, S., Huang, S., Wang, H., Yang, W. and Liu, F. (2016). Improving in-season estimation of rice yield potential and responsiveness to topdressing nitrogen application with Crop Circle active crop canopy sensor. *Precis. Agric*., 17: 136–154.

Chang, L., Peng-Sen, S. and Liu Shi-Rong (2016). "A review of plant spectral reflectance response to water physiological changes," *Chinese Journal of Plant Ecology*, 40(1): 80–91.

Córcoles, J.I., Ortega, J.F., Hernández, D. and Moreno, M.A. (2013). Estimation of leaf area index in onion (Allium cepa L.) using an unmanned aerial vehicle. *Biosyst. Eng*., 115: 31–42.

Garcia-Ruiz, F., Sankaran, S., Maja, J.M., Lee, W.S., Rasmussen, J. and Ehsani, R. (2013). Comparison of two aerial imaging platforms for identification of Huanglongbing-infected citrus trees. *Comput. Electron. Agric*., 91: 106–115

Haboudane, D., Miller, J.R., Pattey, E., Zarco-Tejada, P.J. and Strachan, I.B. (2004). "Hyperspectral vegetation indices and novel algorithms for predicting green LAI of crop canopies: modelling and validation in the context of precision

agriculture," *Remote Sensing of Environment*, 90(3): 337–352.

Hunt, E.R.J., Cavigelli, M., Daughtry, C.S.T., McMurtrey, J.I. and Walthall, C.L. (2005). Evaluation of digital photography from model aircraft for remote sensing of crop biomass and nitrogen status. *Precision Agric*., 6: 359–378.

Kanke, Y., Raun, W., Solie, J., Stone, M. and Taylor, R. (2012). Red edge as a potential index for detecting differences in plant nitrogen status in winter wheat. *J. Plant Nutrition*, 35: 1526–1541.

Liu, H.Q. and Huete, A. (1995). "Feedback based modification of the NDVI to minimize canopy background and atmospheric noise," *IEEE Transactions on Geoscience and Remote Sensing*, 33(2): 457–465.

Liu, K., Yazhen, L.I. and Huiwen, H.U. (2014). Estimating the effect of urease inhibitor on rice yield based on NDVI at key growth stages. *Front. Agric. Sci. Eng*., 1: 150–157.

Liu, X., Ferguson, R.B., Zheng, H., Cao, Q., Tian, Y., Cao, W. and Zhu, Y. (2017). Using an active-optical sensor to develop an optimal NDVI dynamic model for high-yield rice Production (Yangtze, China). *Sensors;* 17: 672.

Li, H., Zhao, C., Yang, G. and Feng, H. (2015). Variations in crop variables within wheat canopies and responses of canopy spectral characteristics and derived vegetation indices to different vertical leaf layers and spikes. *Remote Sens. Environ*., 169: 358–374.

Li, X., Lee, W.S., Li, M., Ehsani, R., Mishra, A.R., Yang, C. and Mangan, R.L. (2012). Spectral difference analysis and airborne imaging classification for citrus greening infected trees. *Comput. Electron. Agric*., 83: 32–46

Mahlein, A.K., Rumpf, T. and Welke, P. (2013). "Development of spectral indices for detecting and identifying plant diseases," *Remote Sensing of Environment*, 128: 21–30.

Mulla, D.J. (2013). "Twenty-five years of remote sensing in precision agriculture: key advances and remaining knowledge gaps," *Biosystems Engineering*, 114(4): 358–371.

Richardson, A.J. and Weigand, C. (1977). "Distinguishing vegetation from soil background information," *Photogrammetric Engineering and Remote Sensing*, p. 43.

Shaver, T.M., Khosla, R. and Westfall, D.G. (2010). Evaluation of two ground-based active crop canopy sensors in maize: Growth stage, row spacing, and sensor movement speed. *Soil Sci. Soc. Am. Journal*. 74: 2101–2108.

Spitkó, T., Nagy, Z., Zsubori, T., Sz˝oke, C., Berzy, T., Pintér, J. and Márton, L. (2016). Connection between normalized difference vegetation index and yield in maize. *Plant Soil Environ.,* 62: 293–298.

Tubaña, B.S., Harrell, D.L., Walker, T., Teboh, J., Lofton, J. and Kanke, Y. (2012). In-season canopy reflectance-based estimation of rice yield response to nitrogen. *Agronomic Journal*, 104: 1604–1611.

Verger, A., Vigneau, N., Chéron, C., Gilliot, J., Comar, A. and Baret, F. (2014). Green area index from an unmanned aerial system over wheat

and rapeseed crops. *Remote Sens. Environ*., 152: 654–664.

Xue, L., Li, G., Qin, X., Yang, L. and Zhang, H. (2014). Topdressing nitrogen recommendation for early rice with an active sensor in south China. *Precis. Agric*. 15: 95–110.

Yao, Y., Miao, Y., Jiang, R., Khosla, R., Gnyp, M.L. and Bareth, G. (2013). Evaluating different active crop canopy sensors for estimating rice yield potential. In Proceedings of the Second International Conference on Agro-Geoinformatics, Fairfax, VA, USA; pp. 538–542.

Zarco-Tejada, P.J., Gonzalez-Dugo, V. and Berni, J.A.J. (2012). Fluorescence, temperature and narrow-band indices acquired from a UAV platform for water stress detection using a micro-hyperspectral imager and a thermal camera. *Remote Sens. Environ*., 117: 322–337.

Zhang, C. and Kovacs, J.M. (2012). "The application of small unmanned aerial systems for precision agriculture: a review," *Precision Agriculture,* 13(6): 693–712.

Zhu, Z., Chen, L., Zhang, J., Pan, Y., Zhu, W. and Hu, T. (2012). Division of winter wheat yield estimation by remote sensing based on MODIS EVI time series data and spectral angle clustering. *Spectroscopy. Spectr. Anal*., 32: 1899–1904.